JCTC Journal of Chemical Theory and Computation

Article

pubs.acs.org/JCTC

Interaction-Strength Interpolation Method for Main-Group Chemistry: Benchmarking, Limitations, and Perspectives

Eduardo Fabiano,*[,†,‡] Paola Gori-Giorgi,[§] Michael Seidl,[§] and Fabio Della Sala[†,‡]

[†]Euromediterranean Center for Nanomaterial Modelling and Technology (ECMT), Istituto Nanoscienze-CNR, Via per Arnesano 16, 73100 Lecce, Italy

[‡]Center for Biomolecular Nanotechnologies@UNILE, Istituto Italiano di Tecnologia (IIT), Via Barsanti, 73010 Arnesano, Italy

[§]Department of Theoretical Chemistry and Amsterdam Center for Multiscale Modeling, FEW, Vrije Universiteit, De Boelelaan 1083, 1081HV Amsterdam, The Netherlands

ABSTRACT: We have tested the original interaction-strength-interpolation (ISI) exchange-correlation functional for main group chemistry. The ISI functional is based on an interpolation between the weak and strong coupling limits and includes exact-exchange as well as the Görling–Levy second-order energy. We have analyzed in detail the basis-set dependence of the ISI functional, its dependence on the ground-state orbitals, and the influence of the size-consistency problem. We show and explain some of the expected limitations of the ISI functional (i.e., for atomization energies) but also unexpected results, such as the good performance for the interaction energy of dispersion-bonded complexes when the ISI correlation is used as a correction to Hartree–Fock.

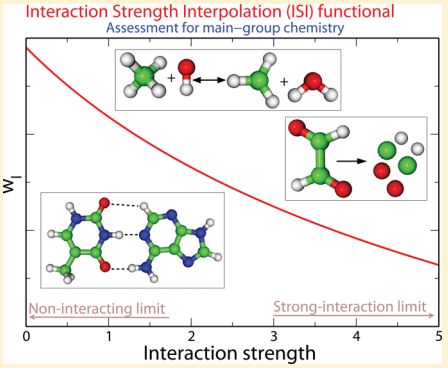

1. INTRODUCTION

Current approximations for the exchange-correlation functional of Kohn–Sham (KS) density functional theory (DFT) work for systems that are weakly or moderately correlated, as they are based on information (exact or approximate) from the weakly correlated regime, when the physical system is not too different from the KS one. The idea of including information from the opposite limit of infinite correlation dates back to Wigner,[1,2] who approximated the correlation energy of the uniform electron gas by interpolating between the limits of zero and infinite interaction strength. Seidl and co-workers[3,4] imported this idea in the framework of KS DFT. They analyzed the structure[3,5] of the DFT limit of infinite coupling strength, proposed a semilocal approximation for it,[6] and built an exchange-correlation (xc) functional by interpolating along the adiabatic connection between zero and infinite interaction strength ("interaction-strength interpolation," or ISI). The original ISI functional interpolates between exact ingredients at weak coupling (exact exchange and second-order perturbation theory) and approximate ingredients at infinite coupling strength, given by the semilocal "point-charge plus continuum" (PC) model.[4,6]

In recent years, the exact solution for the limit of infinite interaction strength in DFT has been derived:[7,8] it is given by a highly nonlocal functional of the density and can be mapped into a mathematical problem appearing in mass-transportation theory.[9,10] Comparison against these exact results showed that the PC model (with a minor readjustment on the next leading term[8]) is a rather accurate approximation for the xc energy at infinite coupling strength,[7,8] while its functional derivative misses the nonlocal features of this limit needed to describe many strong-correlation phenomena in DFT in a *spin-restricted* framework.[11−13] Another approximation for the strong-coupling limit that retains some of its nonlocality (the "nonlocal radius" model, or NLR) has been recently proposed in ref 14 and used by Zhou, Bahmann, and Ernzerhof[15] to construct new xc functionals that use the information at infinite coupling strength.

A formal drawback of the original ISI functional is that it is size consistent only when a system dissociates into equal fragments. This problem is shared by different nonlocal methods in DFT (see, e.g., refs 16 and 17) and in particular by the approximations based on a global interpolation (i.e., performed on quantities integrated over all space) along the adiabatic connection, like the one of ref 18. For the latter, a possible way to restore size consistency in the usual DFT sense[19,20] is to turn to models based on *local* interpolations performed in each point of space,[21] a route that is being presently explored by different authors.[15,22−26] An efficient implementation of the ingredients needed for a local interpolation along the adiabatic connection[22] in the ISI spirit is not yet available, and it is the object of ongoing work.

While a considerable amount of theoretical work on xc functionals that include in an approximate or exact way the strong-interaction limit has been done, benchmarking has been restricted so far to atomization energies,[4,15] ionization potentials,[15] or to simple paradigmatic physical[11,13,27] and

Received: July 18, 2016
Published: September 6, 2016

DOI: 10.1021/acs.jctc.6b00713
J. Chem. Theory Comput. 2016, 12, 4885−4896

chemical[22,28−31] models only. Very little is known about the performance of such functionals for bigger systems and for other chemical and physical properties and about technical aspects such as their sensitivity to reference orbitals and their basis-set dependence.

The purpose of the present work is to fill this gap, by starting from a systematic study of the ISI functional in its original formulation, for which all the ingredients are readily available. This allows us to start to analyze quantitatively which effects are well captured by a functional that includes the strong-coupling limit, together with the practical consequences of the size-consistency error for heterolytic dissociation, as well as to examine restricted versus unrestricted calculations, and other aspects such as sensitivity to the reference orbitals. Our main aim is to provide valuable information for a future generation of functionals based on local interpolations along the adiabatic connection that can include the strong-coupling limit without violating size consistency.[15,22−26]

As we see, our results show some of the expected limitations of the original ISI functional, but also unexpected results, like an excellent performance for the interaction energy of dispersion-bonded complexes that definitely deserves further study.

2. THEORETICAL BACKGROUND

The ISI xc functional[3,4,6] is built by modeling the standard density-fixed linear adiabatic connection integrand $W_\lambda[\rho]$,[32]

$$W_\lambda[\rho] = \langle \Psi_\lambda[\rho]|\hat{V}_{ee}|\Psi_\lambda[\rho]\rangle - U[\rho] \tag{1}$$

where $\Psi_\lambda[\rho]$ is the wave function yielding the density ρ and minimizing $\langle\Psi|\hat{T} + \lambda\ \hat{V}_{ee}|\Psi\rangle$, and $U[\rho]$ is the Hartree (or Coulomb) energy, with a functional form $W_\lambda^{\mathrm{ISI}}[\rho]$ that has the exact weak- and strong-coupling asymptotic behavior,

$$W_{\lambda\to 0}[\rho] = E_x[\rho] + 2\lambda E_{\mathrm{GL2}}[\rho] + \ldots \tag{2}$$

$$W_{\lambda\to\infty}[\rho] = W_\infty[\rho] + \frac{W'_\infty[\rho]}{\sqrt{\lambda}} + \ldots \tag{3}$$

Its final form for the xc energy is obtained as

$$E_{xc}^{\mathrm{ISI}}[\rho] = \int_0^1 W_\lambda^{\mathrm{ISI}}[\rho]d\lambda \tag{4}$$

and reads

$$E_{xc}^{\mathrm{ISI}} = W_\infty + \frac{2X}{Y}\left[\sqrt{1+Y} - 1 - Z\ln\left(\frac{\sqrt{1+Y}+Z}{1+Z}\right)\right] \tag{5}$$

where

$$X = \frac{xy^2}{z^2},\quad Y = \frac{x^2y^2}{z^4},\quad Z = \frac{xy^2}{z^3} - 1 \tag{6}$$

and $x = -4E_{\mathrm{GL2}}$, $y = W'_\infty$, and $z = E_x - W_\infty$. The ISI functional is thus based on four ingredients: two come from the limit of weak interaction of eq 2 expressed in terms of orbital and orbital energies, namely, the exact exchange energy

$$E_x = -\frac{1}{2}\sum_{i,j}\int d\mathbf{r}\int d\mathbf{r}'\frac{\phi_i^*(\mathbf{r})\phi_j^*(\mathbf{r}')\phi_j(\mathbf{r})\phi_i(\mathbf{r}')}{|\mathbf{r}-\mathbf{r}'|} \tag{7}$$

and the Görling−Levy[33] second-order energy

$$E_{\mathrm{GL2}} = -\frac{1}{4}\sum_{abij}\frac{|\langle\phi_i\phi_j||\phi_a\phi_b\rangle|^2}{\epsilon_a+\epsilon_b-\epsilon_i-\epsilon_j} - \sum_{ia}\frac{|\langle\phi_i|\hat{v}_x^{\mathrm{KS}} - \hat{v}_x^{\mathrm{HF}}|\phi_a\rangle|^2}{\epsilon_a-\epsilon_i} \tag{8}$$

where $\langle\cdots||\cdots\rangle$ denotes an antisymmetrized two-electron integral; two are derived from the limit of strong coupling of eq 3: $W_\infty[\rho]$ is the indirect part of the minimum possible expectation value of the electron−electron repulsion in a given density,[7] and $W'_\infty[\rho]$ is the potential energy of coupled zero-point oscillations of localized electrons.[8] They are both highly nonlocal density functionals that are presently expensive to compute exactly.[7,8,13,31,34,35] They are well approximated[7,8] by the semilocal PC model,[6] which we use in this work,

$$W_\infty[\rho] = \int\left[A\rho(\mathbf{r})^{4/3} + B\frac{|\nabla\rho(\mathbf{r})|^2}{\rho(\mathbf{r})^{4/3}}\right]d\mathbf{r} \tag{9}$$

$$W'_\infty[\rho] = \int\left[C\rho(\mathbf{r})^{3/2} + D\frac{|\nabla\rho(\mathbf{r})|^2}{\rho^{7/6}(\mathbf{r})}\right]d\mathbf{r} \tag{10}$$

The parameters $A = -1.451$, $B = 5.317\times10^{-3}$, and $C = 1.535$ are determined by the electrostatics of the PC cell,[6] while the parameter D cannot be derived in the same way, and different choices are possible. For example, we can fix D by requiring that $W'_\infty[\rho]$ be self-interaction free for the H atom density.[6] Another possible choice, which was adopted when the ISI functional was first proposed and tested for atomization energies, is to fix D by requiring that $W'_\infty[\rho]$ be exact for the He atom density.[4] At the time, however, the exact solution for $W'_\infty[\rho]$ was not available, and the accurate $W'_\infty[\rho]$ for He was estimated from a metaGGA functional. A few years later, when the exact $W'_\infty[\rho]$ has been evaluated for several atomic densities, it has been found that the metaGGA values were not accurate enough.[8] The parameter D has then been changed and fixed by using the exact $W'_\infty[\rho]$ for the He atom. This choice, corresponding to $D = -2.8957\times10^{-2}$, improves significantly the agreement between the PC model for $W'_\infty[\rho]$ and the exact values for several atomic densities,[8] and it is the one we use in this work.

To see how the limits of eqs 2 and 3 are included in the ISI functional of eq 5, we can expand $E_{xc}^{\mathrm{ISI}}[\rho]$ in a series for small E_{GL2},

$$E_{xc}^{\mathrm{ISI}}|_{E_{\mathrm{GL2}}\to 0} = E_x + E_{\mathrm{GL2}} + \frac{4}{3(E_x - W_\infty)}E_{\mathrm{GL}\,2}^2 + \ldots \tag{11}$$

showing that ISI includes the exact-exchange and recovers second-order perturbation theory.

The opposite limit of strong correlation is normally signaled by the closing of the energy gap between the highest occupied molecular orbital (HOMO) and the lowest unoccupied molecular orbital (LUMO), which usually makes appear a broken symmetry solution with lower energy. If we do not allow symmetry breaking, the gap closes, implying that $E_{\mathrm{GL2}} \to -\infty$ and

DOI: 10.1021/acs.jctc.6b00713
J. Chem. Theory Comput. 2016, 12, 4885−4896

$$E_{xc}^{\mathrm{ISI}}|_{E_{\mathrm{GL2}}\to-\infty} = W_\infty + 2W'_\infty - \frac{2W'^2_\infty}{E_x - W_\infty}\ln\left(1 + \frac{E_x - W_\infty}{W'_\infty}\right) \quad (12)$$

The first two terms, $W_\infty[\rho] + 2\,W'_\infty[\rho]$, give the xc energy in the limit of strong coupling, which is the sum of a purely electrostatic indirect part ($W_\infty[\rho]$) and electronic zero point oscillations (the factor two in front of $W'_\infty[\rho]$ accounts for the zero point kinetic energy[8] and comes from the integration of the term $\sim \lambda^{-1/2}$ in eq 3). The last term in eq 12 is dependent on the interpolating function and can change if we choose different forms (see, e.g., the ones of refs 8 and 36).

If the four ingredients E_x, E_{GL2}, W_∞, and W'_∞ are size consistent, then the ISI xc functional is size consistent only when a system dissociates into equal fragments, as it can be easily derived from eq 5. A detailed and quantitative analysis of the problem is reported in Section 5.1.

We should notice, however, that within the less usual restricted framework for open shell fragments, which seems crucial to capture strong correlation without introducing artificial magnetic order and is the present focus of a large theoretical effort,[24−26,37] size consistency of the E_x and E_{GL2} is lost,[38] and usually $E_{\mathrm{GL2}} \to -\infty$ at dissociation. In this case, the ISI xc functional stays finite and tends to the expression of eq 12). In this work, we have tested the ISI functional following the standard procedure of allowing spin-symmetry breaking (for a very recent review on spin symmetry breaking in DFT see ref 39), and we discuss only briefly paradigmatic calculations (the H_2 and N_2 dissociation curves) in a spin-restricted formalism. It is however clear from eq 12 that the ISI xc functional is not able to dissociate a single or multiple bond properly in a spin-restricted framework since eq 12 will not provide the right energy in this limit. The ISI accuracy in the usual unrestricted KS (or Hartree−Fock) formalism are less easy to predict, and its analysis is the main object of this work.

3. COMPUTATIONAL DETAILS

The calculations with the ISI xc functional defined by eqs 5−10 have been performed in a post-self-consistent-field (post-SCF) fashion, using reference orbitals and densities obtained from different methods, namely, DFT calculations using the Perdew−Burke−Ernzerhof (PBE[40]), the hybrid PBE (PBE0[41,42]), and the hybrid Becke-half-and-half (BHLYP[43−45]) exchange-correlation functionals and the localized Hartree−Fock (LHF) effective exact exchange method[46] and the Hartree−Fock (HF) method.

In different parts of the paper, we consider the ISI correlation energy, which is defined, as usual in the DFT framework,[47] as $E_c^{ISI} = E_{xc}^{ISI} - E_x$, where E_{xc}^{ISI} and E_x are the ISI xc energy (eq 5) and the exact exchange energy (eq 7), respectively. Note that this definition of the ISI correlation energy is well justified since the ISI xc functional includes the full exact exchange.[4]

Unless otherwise stated, all energies have been extrapolated to the complete basis set limit as described in Section 3.1, using data from calculations performed with the Dunning basis set family cc-pVnZ (n = 2,...,6).[48−51] For spin-polarized systems, a UHF formalism has been employed in the self-consistent calculations. All calculations have been performed using a development version of the TURBOMOLE program package.[52,53]

To assess the performance of the ISI xc functional in practical applications, we considered the following set of tests:

Thermochemistry Data Set. This contains atomization energies (AE6,[54,55] G2/97[56,57]), ionization potentials (IP13[58]), electron and proton affinities (EA13[58] and PA12[59]), barrier heights (BH76[59−62] and K9[55,63]), and reaction energies (BH76RC[59−62] and K9[55,63]) of small main-group molecules.

Noncovalent Interactions Data Set. This contains interaction energies of noncovalent complexes having hydrogen bond (HB6[64]), dipole−dipole (DI6[64]), charge-transfer (CT7[64]), dihydrogen-bond (DHB23[65]), and various (S22[66,67]) character.

3.1. Basis Set Dependence. The ISI correlation energy formula contains the GL2 correlation energy of eq 8. The latter is well known to exhibit a relevant basis set dependence as well as a slow convergence to the complete basis set (CBS) limit. Thus, a similar behavior can be expected also for the ISI correlation energy. Nevertheless, because the ISI energy also includes other input quantities, whose basis set dependence is different from that of GL2, and because all the input quantities enter nonlinearly in the ISI formula, it is not simple to derive analytically the ISI basis set dependence. This situation is depicted in Figure 1, where we report, for the F atom, the basis set evolution of the different input quantities of the ISI energy as well as of the ISI correlation energy itself.

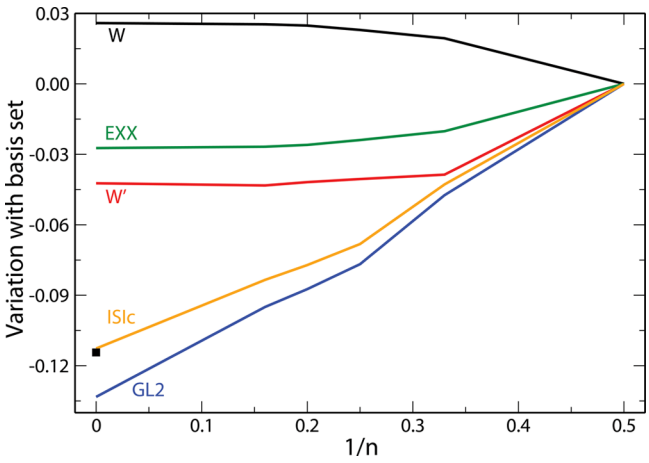

Figure 1. Variation with the basis set (cc-pVnZ) of the various input quantities (in Ha) used to compute the ISI correlation energy, here for the F atom. The black square at $1/n = 0$ indicates the extrapolation obtained applying eq 13.

For this reason, it is not convenient trying to derive the ISI basis set behavior starting from the assumed behavior of GL2 and other input quantities, as given by popular basis set interpolation−extrapolation formulas.[68−73] Instead, it is more practical to consider the basis set evolution of the ISI correlation energy as a whole. To this end, in analogy with previous works on basis set extrapolation,[69,70,73] we consider the following ansatz

$$E_c^{\mathrm{ISI}}[n] = E_c^{\mathrm{ISI}}[\infty] + An^{-\alpha} \quad (13)$$

where the notation $[n]$ indicates that the energy is computed with an n-zeta quality basis set (here, specifically, the cc-pVnZ basis set), A is a system-dependent constant, and α is an exponent determining the strength of the basis set dependence. Equation 13 provides an accurate fit for the ISI correlation energies of different systems as we show in Figure 2 where we

DOI: 10.1021/acs.jctc.6b00713
J. Chem. Theory Comput. 2016, 12, 4885−4896

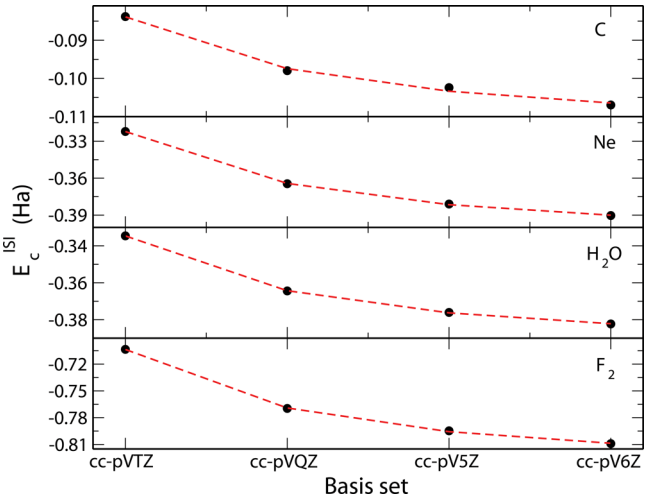

Figure 2. Evolution of the ISI correlation energy of different test systems with basis set. The red dashed lines denote interpolations obtained using eq 13.

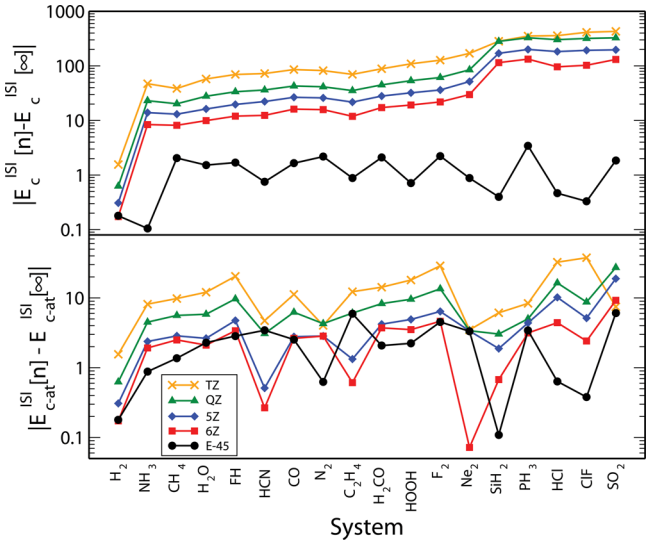

Figure 3. Deviations of the ISI correlation energies (in mHa) computed with various basis sets from the benchmark CBS ones. Absolute correlation energies (upper panel) and atomization correlation energies (lower panel).

report, for some example systems, the ISI correlation energies computed with several basis sets and the corresponding fit obtained from eq 13. Note also that, as shown in Figure 1, eq 13 reproduces correctly the CBS extrapolated value of the ISI correlation energy as computed using the extrapolated values of all input ingredients.

Use of eq 13 allows us to obtain accurate CBS-ISI energies. However, a more practical approach is to use eq 13 into a two-point scheme[68,69,73] to have the extrapolation formula

$$E_c^{\mathrm{ISI}}[\infty] = \frac{E_c^{\mathrm{ISI}}[n]n^\alpha - E_c^{\mathrm{ISI}}[m]m^\alpha}{n^\alpha - m^\alpha} \quad (14)$$

where n and m label two selected basis sets. In this work, we considered n = 5 and m = 4 (for basis sets smaller than cc-pVQZ we could not avoid numerical noise in some cases) and fixed the parameter α = 2.2475 by fitting to the accurate CBS ISI correlation energies of atoms He−Ar, obtained by applying eq 13 to the full set of data corresponding to n = 4,...,6. The calculations have been performed in a post-SCF fashion using LHF orbitals (almost identical results have been obtained using Hartree−Fock orbitals). Note that the optimized value of α is a bit larger than the corresponding ones obtained in ref 74 for MP2 and CCSD (1.91 and 1.94, respectively). This indicates that the ISI correlation converges slightly faster than the MP2 and CCSD ones to the CBS limit, possibly because it benefits from the fast convergence of the pure density-dependent contributions.

A test of eq 14 is reported in Figure 3 where we show the errors on ISI absolute correlation energies (upper panel) and atomization correlation energies (lower panel) computed with different basis sets, as compared to CBS reference ones, i.e., $E_c^{\mathrm{ISI}}[\infty]$ of eq 13 fitted to the data with n = 3,...,6 with eq 13. The results obtained using eq 14 are labeled as E-45 in the figure. For the absolute correlation energies, we see that even at the cc-pV6Z level errors of about 10 mHa can be expected, while only energies obtained via the extrapolation formula of eq 14 show accuracies of about 1 mHa. For the atomization correlation energies, we deal with energy differences. Therefore, error compensation effects are quite relevant, especially for the smallest basis sets. Thus, the errors are close or lower than 10 mHa even for the cc-pVTZ basis set. Nevertheless, accurate results (about 1 mHa) can be obtained systematically only using at least a cc-pV5Z basis set or, even better, via the extrapolation formula of eq 14.

4. RESULTS

4.1. Role of the Reference Orbitals. The ISI correlation functional is a complicated orbital-dependent nonlinear functional. Thus, a stable self-consistent implementation is a complicated task going beyond the scope of this paper. Here, the ISI correlation is employed in a post-SCF scheme, where the ground-state orbitals and density are computed using a simpler approach and then used to evaluate the ISI correlation (and also the exact exchange contribution).

The relevance of the reference density and orbitals for different DFT calculations has been pointed out in several works in the literature.[75,76] Therefore, it appears important to assess the reliability of different reference orbitals for the calculation of the ISI correlation. Furthermore, because the ISI functional is including the GL2 correlation energy as an input ingredient, the orbital energies, and in particular the HOMO−LUMO gap, can be expected to play a major role (see discussion in Section 5.2). Hence, we take into account reference ground-state orbitals computed with the generalized gradient xc approximation of Perdew−Burke−Ernzerhof (PBE),[40] with the hybrid functionals PBE0[41,42] and BH-LYP,[43−45] which include 25% and 50% of exact exchange, respectively, with the optimized effective potential named localized Hartree−Fock (LHF)[46] and with the Hartree−Fock (HF) method. Note that the inclusion of larger fractions of nonlocal Hartree−Fock exchange yields increasingly large HOMO−LUMO gaps, which are also effectively used in double-hybrid functionals.[77] We remark that the LHF method is instead a *de facto* exact exchange Kohn−Sham approach. As such, it gives significantly smaller values of the HOMO−LUMO gap than Hartree−Fock. Moreover, it may provide a better approximation of the self-consistent ISI ground-state density and orbitals than approximate functionals or the Hartree−Fock method (we recall that in general correlation contributions to the density and orbitals are rather small[78−81]).

DOI: 10.1021/acs.jctc.6b00713
J. Chem. Theory Comput. 2016, 12, 4885−4896

Table 1. Total Correlation Energies (in mHa, with opposite sign) from Semilocal DFT Functionals (LYP, PBE, PBEloc, all using PBE orbitals), ISI, and GL2 Methods Calculated Using Different Reference Ground-State Orbitals[a]

correlation:	LYP	PBE	PBEloc	ISI					GL2					
orbitals:	PBE	PBE	PBE	PBE	PBE0	BHLYP	LHF	HF	PBE	PBE0	BHLYP	LHF	HF	ref
closed-shell atoms														
He	43.7	41.1	33.8	44.3	40.9	38.3	41.8	34.5	52.3	46.9	42.8	48.4	37.4	42
Ne	383.1	347.1	358.3	433.6	400	375.8	406.5	338	500.3	452.9	419.8	462.6	370.1	391
Ar	751.5	704.4	757.4	709.4	658.3	618.8	696.2	556.5	723.1	663.1	619.8	708	558.2	723
ME	7.4	−21.1	−2.2	10.4	−18.9	−41.0	−3.8	−75.7	39.9	2.3	−24.5	21.0	−63.4	
MAE	12.7	21.1	25.1	19.5*	24.9*	41.0*	14.2*	75.7	39.9	42.2	44.3	31.0	63.4*	
open-shell atoms														
C	158.3	144.3	139.8	145.8	129.7	118.2	138	102.1	178.6	152.4	135	166.3	112.7	156
N	191.9	179.9	176.4	181.9	166.2	154.4	172.5	136.6	217.3	192.9	175.6	203.2	151.3	188
O	256.6	235.2	234.8	251.1	230.5	215.4	237	191.7	303.2	270.4	247.7	281.4	214.2	255
F	321	292.6	297.4	328.4	303.1	284.6	309.6	255.4	398.4	357.7	329.5	368.7	287.6	323
Si	529.2	484.2	516.8	515.3	474.5	444.4	498.9	395.2	518.3	470.3	446.3	508.8	393.5	505
P	566.4	526.5	564	544.4	504.1	473.6	531.6	424.5	553.3	505.5	480.6	543.3	426.7	540
S	627.7	584.1	626.1	592.1	547.5	514.4	575.4	459.8	600.9	546.9	517.9	585.8	456.6	603
Cl	689.7	644.5	691.6	640.2	592.8	557	623.8	499.3	658.5	600.1	559.3	638.6	501.3	664
ME	13.4	−17.8	1.6	−4.4	−35.7	−59.0	−18.4	−96.2	24.3	−17.2	−42.8	7.8	−86.3	
MAE	13.9	17.8	20.0	9.4*	35.7	59.0	18.4	96.2	26.2	31.0*	44.4*	18.4	86.3*	
closed-shell molecules														
H_2	38.2	42.9	37.4	38.4	35	32.2	36.9	28	53.2	46.3	41.2	50.4	34.3	41
NH_3	318	314.2	310.8	371.2	337.2	312.1	354.7	271.9	463.3	406.7	367.6	436.3	309.4	340
CH_4	295	300	292.5	315.8	287.3	265.1	304.5	230.2	391.5	344.9	310.8	373.5	261.1	299
H_2O	340.4	324.8	325.5	416.1	378.1	350.7	393.8	307	514.7	452.5	410.2	478.7	347.6	371
FH	362.2	335.1	340.4	439.6	400.8	373	412.1	329.6	528.9	469.1	428.2	486.8	368.2	389
HCN	464.8	439.7	437.8	604.4	536.8	488	561	414.3	773.8	655.2	577.1	714.7	470.1	515
CO	485.2	448.4	451	627.4	558.1	508	586.3	434.1	787.5	670.7	593	718.2	487.9	535
N_2	484.2	451.5	452.5	644.5	574.5	523.8	612.4	446.1	821	699.3	618.7	766.2	505.8	549
C_2H_4	498.7	493.7	486.8	568.9	511.7	468.6	543.6	402.7	709.3	614.6	548.4	668.3	454.8	480
H_2CO	540.7	514.4	514.6	673.8	602.9	550.9	632.4	473.6	844.5	725.1	644.6	775.3	534.3	586
HOOH	636.7	598.5	604.7	818.2	736.2	677.4	775.1	586.3	1023.1	885.6	794.1	951.3	663.2	711
F_2	675.5	612.7	627	882.2	790.8	727	833	631.2	1081	934.4	838.7	1003.2	705.3	757
SiH_2	598.3	553.8	582.6	609.4	553.8	513.4	586.8	452.5	615.9	548.8	512.1	588.2	455.3	567
PH_3	676.7	642.7	677	696.6	637.1	591.4	675.6	522.3	719.9	646.1	591.4	693.8	522.8	652
SO_2	1257.5	1171.3	1227.6	1570.3	1399.7	1278.6	1467.5	1103.5	1813.3	1559.2	1391.1	1659.4	1164.5	1334
ClF	1047.6	970.8	1028.1	1158.3	1049.8	971.4	1104	855.2	1262.2	1118.7	1019.3	1190.6	878.6	1063
HCl	727.6	686.2	733.5	720.2	664	621.4	703.9	554.7	740.9	673.1	623.1	721.6	557.5	707
ME	−26.4	−58.5	−45.1	74.1	9.3	−37.8	40.4	−109.0	191.1	91.4	24.3	140.0	−69.1	
MAE	37.6	60.5	53.8	74.4*	21.6*	37.8*	41.3*	109.0	191.1	98.3	52.9	140.0	69.1*	
overall statistics														
ME	−11.4	−42.9	−27.1	44.9	−6.6	−44.2	18.9	−101.8	127.2	50.8	−0.1	89.5	−73.4	
MAE	28.2	44.1	41.1	49.9*	26.0*	44.2*	31.8*	101.8	127.8	73.0	49.6	93.6	73.4*	

[a]Reference data are taken from ref 86. The last lines report the mean error (ME) and the mean absolute error (MAE) for each case; a star is appended to the MAEs to indicate, for each choice of the reference orbitals, the best method between ISI and GL2.

Anyway, we cannot exclude that the self-consistent ISI potential may display non-negligible differences with respect to the LHF (or the exact exchange) one. These differences might concern especially a reduction of the HOMO−LUMO gap that will induce a lowering of the total xc energy (note, however, that for the ISI functional a complete collapse of the HOMO−LUMO gap is not likely because, unlike in the GL2 case,[82] the large increase in kinetic energy associated with it cannot be compensated by the divergence of the correlation energy, which is bounded from below in ISI) and cases where static correlation is rather important.

In Table 1, we report the ISI correlation energies (in absolute value) obtained using different reference ground-state densities and orbitals (see also Figure 4). The corresponding GL2 energies are also listed in order to compare to the ISI ones (a star is appended to the mean absolute errors reported in Table

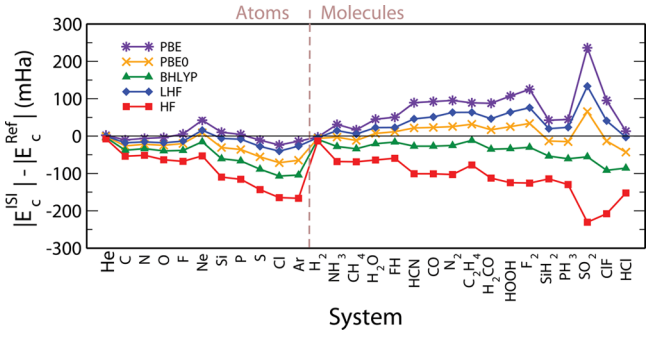

Figure 4. Errors on absolute ISI correlation energies (mHa) calculated using different reference ground-state densities and orbitals.

DOI: 10.1021/acs.jctc.6b00713
J. Chem. Theory Comput. 2016, 12, 4885−4896

Table 2. Correlation Atomization Energies (mHa, with opposite sign) from Semilocal DFT Functionals (using PBE orbitals) As Well As ISI and GL2 Methods Calculated Using Different Reference Ground-State orbitals[a]

correlation:	LYP	PBE	PBEloc	ISI					GL2					
orbitals:	PBE	PBE	PBE	PBE	PBE0	BHLYP	LHF	HF	PBE	PBE0	BHLYP	LHF	HF	ref
H_2	38.2	42.9	37.4	38.4	35.0	32.2	36.9	28.0	53.2	46.3	41.2	50.4	34.3	41.0
NH_3	126.1	134.3	134.4	189.3	171.0	157.7	182.2	135.3	246.0	213.8	192.0	233.1	158.1	152.0
CH_4	136.7	155.7	152.7	170.0	157.6	146.9	166.5	128.1	212.9	192.5	175.8	207.2	148.4	143.0
H_2O	83.8	89.6	90.7	165.0	147.6	135.3	156.8	115.3	211.5	182.1	162.5	197.3	133.4	116.0
FH	41.2	42.5	43.0	111.2	97.7	88.4	102.5	74.2	130.5	111.4	98.7	118.1	80.6	66.0
HCN	114.6	115.5	121.6	276.7	240.9	215.4	250.5	175.6	377.9	309.9	266.5	345.2	206.1	171.0
CO	70.3	68.9	76.4	230.5	197.9	174.4	211.3	140.3	305.7	247.9	210.3	270.5	161.0	124.0
N_2	100.4	91.7	99.7	280.7	242.1	215.0	267.4	172.9	386.4	313.5	267.5	359.8	203.2	173.0
C_2H_4	182.1	205.1	207.2	277.3	252.3	232.2	267.6	198.5	352.1	309.8	278.4	335.7	229.4	168.0
H_2CO	125.8	134.9	140.0	276.9	242.7	217.3	257.4	179.8	362.7	302.3	261.9	327.6	207.4	175.0
HOOH	123.5	128.1	135.1	316.0	275.2	246.6	301.1	202.9	416.7	344.8	298.7	388.5	234.8	201.0
F_2	33.5	27.5	32.2	225.4	184.6	157.8	213.8	120.4	284.2	219.0	179.7	265.8	130.1	111.0
SiH_2	69.1	69.6	65.8	94.1	79.3	69.0	87.9	57.3	97.6	78.5	65.8	79.4	61.8	62.0
PH_3	110.3	116.2	113.0	152.2	133.0	117.8	144.0	97.8	166.6	140.6	110.8	150.5	96.1	112.0
SO_2	116.6	116.8	131.9	476.0	391.2	333.4	418.1	260.3	606.0	471.5	377.8	510.8	279.5	221.0
ClF	36.9	33.7	39.1	189.7	153.9	129.8	170.6	100.5	205.3	160.9	130.5	183.3	89.7	76.0
HCl	37.9	41.7	41.9	80.0	71.2	64.4	80.1	55.4	82.4	73.0	63.8	83.0	56.2	43.0
ME	−35.8	−31.8	−29.0	82.0	54.0	34.0	68.2	5.2	137.8	91.9	60.4	114.8	20.9	
MAE	38.3	39.3	35.3	82.3*	54.7*	35.1*	68.7*	12.7*	137.8	91.9	60.5	114.8	23.6	

[a]Reference data are taken from ref 86. The last lines report the mean error (ME) and the mean absolute error (MAE) for each case; a star is appended to the MAEs to indicate, for each choice of the reference orbitals, the best method between ISI and GL2.

1 to indicate, for each choice of the reference orbitals, the best method between ISI and GL2). We recall that the GL2 and ISI results are extrapolated to the CBS limit, as described in eq 14 (for GL2, we used eq 13 with cc-pVQZ and cc-pV5Z results and the optimized value $\alpha = 2.8$). As already discussed, the expected accuracy of such an extrapolation is $\lesssim$10 mHa (this explains the fact that for a few cases, e.g., Si, S, and SiH_2 using PBE0 orbitals, we have $|E_c^{ISI}| > |E_c^{GL2}|$, whereas by construction it holds $|E_c^{ISI}| \leq |E_c^{GL2}|$). Table 1 also shows the correlation energies computed with some popular semilocal generalized-gradient approximation (GGA) functionals (namely, the Lee−Yang−Parr (LYP),[45] PBE, and PBE with localization (PBEloc)[83] functionals), in order to provide a comparison for the expected accuracy of standard DFT calculations. The correlation energies for GGA functionals have been computed using the cc-pV5Z basis set and the PBE self-consistent orbitals. Note that GGA correlation functionals include only dynamical correlation,[84,85] whereas the ISI method includes both dynamical and static correlation.

We see that the results depend rather importantly on the used reference ground-state orbitals. This indicates that any non-self-consistent use of the ISI functional must be considered with the due caution, while only self-consistent calculations could give definitive information on the real quality of the ISI energy. However, the self-consistent implementation of the ISI functional is an extremely hard task. On the other hand, using reference orbitals which are simpler to compute, in order to evaluate ISI functional non-self-consistently, may offer a more pragmatic approach that can still provide interesting information on this method. For this reason, we consider this analysis in the following.

A first inspection of the overall results, i.e., the MAE in the overall statistics at the bottom of the table, shows that the best ISI results are found using PBE0 and LHF orbitals (overall mean absolute errors (MAEs) of 26.0 and 31.8 mHa, respectively). We remark that these results are of similar quality as those of the semilocal DFT functionals: the MAE of the best GGA functional (LYP) is 28 mHa. On the other hand, the use of the PBE orbital leads to overestimated absolute ISI correlation energies, while the use of HF or BH-LYP orbitals yields largely underestimated absolute energies. Similar trends are obtained for the underlying GL2 (MP2 in the case of HF) correlation energies. It is interesting to see that ISI strongly improves over GL2 for PBE, PBE0, and LHF; an opposite trend is found for HF, while no relevant differences are found for BH-LYP.

A more detailed analysis of the different systems can be obtained by inspecting the statistics reported for different classes of systems as well as inspecting Figure 4 which reports the errors on the absolute ISI correlation energies for all the systems. The plot clearly shows that the use of Hartree−Fock orbitals leads to an underestimation of the absolute correlation for all systems. Instead, when LHF and PBE orbitals are considered, atomic correlation energies are computed with quite good accuracy, but molecular correlation energies are significantly overestimated. This finding has an important effect on the calculation of atomization correlation energies as shown in Table 2. In this case the smaller errors are found for HF-based calculations, which benefit from a large error cancellation effect; indeed, as shown in Figure 4, molecules and atoms are underestimated by about the *same* quantity. On the contrary, for all other reference orbitals, an important overestimation of the absolute ISI correlation energy is observed. Note that, in any case, the ISI correlation atomization energies computed for the present test set are always better than the corresponding GL2 correlation atomization energies, yielding MAEs of 138.5, 92.5, 62.4, 116.5, and 23.7 mHa for PBE, PBE0, BHLYP, LHF, and HF orbitals, respectively. Moreover, the HF-ISI results are also almost 3 times better than those obtainable by semilocal

DOI: 10.1021/acs.jctc.6b00713
J. Chem. Theory Comput. 2016, 12, 4885−4896

Table 3. Total Atomization Energies (mHa, with opposite sign) Form Semilocal DFT Functionals (using PBE orbitals) As Well As from ISI Methods Calculated Using Different Reference Ground-State Densities and Orbitals. Reference data are taken from ref 86[a]

method:	HF+LYP	HF+PBE	HF+PBEloc	ISI					
orbitals:	PBE	PBE	PBE	PBE	PBE0	BHLYP	LHF	HF	ref
H_2	172.3	164.5	163.8	171.2	168.2	165.5	170.5	161.6	174.5
NH_3	446.4	436.6	443.9	506.1	489.8	476.8	500.4	455.5	475.5
CH_4	660	655	661.8	689.3	678.7	668.9	687.4	651.4	626
H_2O	332.1	325.9	331.9	411	395	383	404	363.6	371
HF	195.6	190.9	193.9	264.2	251.6	242.6	256.6	228.7	216.4
HCN	431.8	426.7	435.2	586.1	554	530.4	459.3	492.7	496.9
CO	348.5	347	354.6	500.9	471.8	450.9	486	418.5	413.8
N_2	284.3	275.6	283.6	457.4	422.2	396.9	446.5	356.7	363.7
C_2H_4	864.6	863.6	875.6	951.6	930.3	912.4	945.7	881	898.8
H_2CO	536	533.1	543.1	676	646.9	625	662.4	590	596.7
HOOH	333.9	326.7	338.4	516.7	481	454.8	505	413.4	428.9
F_2	25.8	31.8	27.1	156.9	120.3	96.5	146.9	61.1	62.5
SiH_2	245.5	233.9	235.1	265.1	252.7	244.4	261.7	233.6	242.9
PH_3	385.2	373.1	377.2	418.2	402.8	390.5	414.2	372.7	387.2
SO_2	290.1	290.4	305.4	624.6	551.3	502.3	580.7	433.9	414.2
ClF	50.5	47.3	52.6	193.8	162.4	141.8	178.3	114	100.1
HCl	160.6	158.4	161	202.4	194	187.3	202.3	178.1	171.2
ME	−42.9	−48.4	−41.8	+67.7	+43.1	+25.3	+51.0	−2.0	
MAE	47.2	51.8	46.0	68.1	43.8	26.3	55.9	11.7	

[a]The last lines report the mean error (ME), the mean absolute error (MAE), and the mean absolute relative error (MARE) for each case. 1mHa = 0.62751 kcal/mol.

DFT functionals (the best being PBEloc with a MAE of 36 mHa).

4.2. Total Atomization Energies. In Table 3, we report the total atomization energies. We compare the ISI results to HF+GGA correlation approaches. Note that in the latter methods no error cancellation between exchange and correlation occurs, and static correlation is not considered.[84,85] Thus, HF+GGA calculations give much worse results than conventional GGA xc approaches. However, here they can be used to assess the quality of the ISI results. ISI-HF has an MAE of only 11.7 mHa which is 4 times better than HF+GGA. Conversely, ISI-LHF largely overestimates atomization energies, yielding an absolute accuracy close to the HF+GGA (which, on the other hand, underestimates the atomization energies.[83])

We note that the present results for ISI atomization energies are slightly different from the ones reported in the original ISI publication.[4] This is due to the different choice of the parameter D in eq 10, which has been fixed here by using the exact value of $W'_\infty[\rho]$ for the He atom density[8] instead of the one estimated from a metaGGA functional used in ref 4, and due to the different basis set used (recall that in the present work we used extrapolation toward the complete basis set limit).

4.3. Main-Group Chemistry Benchmark. To assess the practical applicability of the ISI functional to main-group chemistry, we have performed a series of tests involving different properties of interest for computational chemistry. We have restricted our study to ISI calculations employing HF and LHF reference orbitals (hereafter denoted as ISI-HF and ISI-LHF, respectively). This choice was based on the fact that, as explained in Section 4.1, ISI-HF is expected to yield the best performance for these tests (according to the results of Table 2), while ISI-LHF provides the best approximation for the performance of self-consistent ISI calculations. For comparison, we report also the MP2 and B2PLYP[77] results, which are based on GL2 energies, as well as the performance of calculations using the popular PBE functional[40] and of the Hartree−Fock exchange coupled with the semilocal PBEloc correlation[83] (HF+PBEloc). The latter is a simple approach adding semilocal dynamical correlation to Hartree−Fock and can give information on the possible accuracy of "standard" DFT methods when used together with exact exchange; we remark anyway that much improved results can be obtained by more sophisticated DFT approaches including static and/or strong correlation treatments.[24,87]

In the upper part of Table 4, we report the mean absolute errors (MAEs) for several standard tests concerning thermochemical properties. In the last line of Table 4, we report, for each method X, the relative mean absolute error (RMAE) with respect MP2, i.e.,

$$RMAE^X = \sum_i \frac{MAE_i^X}{MAE_i^{MP2}} \tag{15}$$

where i indicates the different tests.

The results clearly show that ISI-LHF often gives the largest MAEs, with a RMAE of 4.1. Significantly better results are obtained by ISI-HF calculations (RMAE = 1.7). However, the performance for barrier heights (BH76 and K9) is quite poor and even worse than that obtained by adding a simple semilocal correlation to Hartree−Fock.[83,88] We note also that for this property Hartree−Fock- and LHF-based ISI calculations yield a quite similar performance. On the other hand, ISI-HF yields the best results for the PA13 test and the S22 test.

When the focus is on noncovalent interactions (bottom part of Table 4), ISI-HF performs quite well for both hydrogen bond (HB6) and dipole−dipole (DI6) interactions having a

DOI: 10.1021/acs.jctc.6b00713
J. Chem. Theory Comput. 2016, 12, 4885−4896

Table 4. Mean Absolute Errors (kcal/mol) on Several Tests As Obtained from ISI Calculations Using LHF and HF Orbitals[a]

test	PBE	HF+PBEloc	MP2	B2PLYP	ISI-HF	ISI-LHF
thermochemistry						
AE6	13.3	24.0	9.6	**1.6**	10.0	43.4
G2/97	14.7	26.3	12.3	**4.0**	15.9	53.1
IP13	3.3	7.0	2.2	**1.9**	3.0	6.0
EA13	**2.8**	9.0	3.4	4.1	5.9	9.3
PA12	2.2	6.6	1.0	1.4	**0.9**	2.6
K9	7.4	4.3	4.1	**1.6**	7.2	8.5
BH76	9.7	6.8	5.2	**2.2**	10.1	11.7
BH76RC	4.3	6.9	3.9	**1.2**	7.0	16.4
noncovalent interactions						
HB6	**0.4**	1.7	**0.4**	**0.4**	0.7	1.1
DI6	**0.4**	**0.4**	0.5	0.5	0.8	3.3
CT7	2.3	1.1	0.8	**0.6**	2.2	7.5
DHB23	1.0	1.0	1.3	**0.5**	5.1	11.0
S22	2.7	1.9	1.2	1.9	**0.4**	1.5
statistics						
RMAE	1.50	2.31	1.00	**0.75**	1.71	4.14

[a]PBE, HF+PBEloc, MP2, and B2PLYP results are reported for comparison. The best (worst) result for each test is in bold (underlined). The last line reports the relative MAE with respect MP2 (eq 15).

comparable accuracy as MP2 and B2PLYP. The ISI-HF functional outperforms other approximations for the S22 test, which contains different kinds of biology relevant noncovalent complexes having hydrogen-bond, dipole–dipole, and dispersion character.

4.4. A Closer Look at Dispersion Complexes. The small error for the S22 test set suggests that ISI-HF may be more accurate than other approaches (e.g., B2PLYP) in the description of dispersion complexes. As further evidence, we report in Figure 5 the signed error obtained from ISI-HF, MP2, and B2PLYP in the calculation of the interaction energy of a collection of different dispersion complexes, which includes the dispersion-dominated S22 cases as well as additional test cases from the literature.[89−92] It can be seen that, indeed, ISI-HF results are always very accurate (≲1 kcal/mol), whereas for the

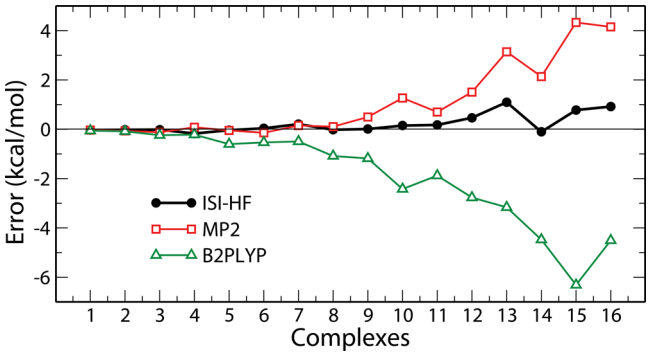

Figure 5. Signed errors (kcal/mol) in the calculation of the interaction energy of different dispersion complexes (1: He–Ne, 2: Ne–Ne, 3: CH_4–Ne, 4: CH_4–F_2, 5: CH_4–CH_4, 6: C_6H_6–Ne, 7: CH_2–CH_2, 8: C_2H_4–C_2H_4, 9: C_6H_6–CH_4, 10: C_6H_6 sandwich dimer, 11: C_6H_6 T-shaped dimer, 12: C_6H_6 displaced dimer, 13: pyrazine-dimer, 14: uracil stacked dimer, 15: adenine–thymine stacked dimer, and 16: indole–benzene stacked dimer).

dimers of aromatic molecules MP2 (B2PLYP) largely overestimate (underestimate) the interaction energy.

In Figure 6, we also report the interaction energy curves for Ne–Ne and C_2H_4–C_2H_4, which show again that ISI-HF

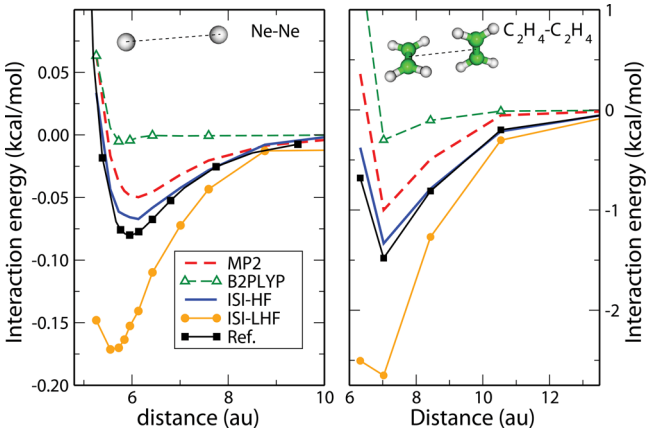

Figure 6. Interaction energy curves for Ne–Ne and C_2H_4–C_2H_4. All energies have been corrected for the basis-set superposition error. Reference values for Ne–Ne and C_2H_4–C_2H_4 have been taken from refs 92 and 93, respectively.

accurately captures dispersion interactions. Further analysis and discussion of these results are reported in Section 5.3.

4.5. Static orrelation. One of the purposes of including the strong-coupling limit into approximate functionals is the hope to capture static correlation without resorting to symmetry breaking. However, it is already clear from eq 12 that the ISI functional will not dissociate correctly a single or multiple bond in a restricted framework. In fact, as the bond is stretched, the ISI xc energy of eq 12 will be quite different than the one for the two equal open shell fragments. The problem is that only the electrons involved in the bonds should be strongly correlated. The rest of the fragment should be in the usual weak or intermediate correlation regime, but the global interpolation makes the whole fragment be in the strong-coupling regime. A local interpolation might fix this issue, but it needs to be constructed carefully.[22]

An exception is the H_2 molecule for which all the electrons are involved in the bond. Indeed, Teale, Coriani, and Helgaker[28] had found a very good agreement between the ISI model for the adiabatic connection curve (in a restricted framework), and their accurate results in the case of the H_2 molecule dissociation, when the bond is stretched up to 10 bohr. Their study used full configuration-interaction (FCI) densities and the corresponding KS orbitals and orbital energies from the Lieb maximization procedure as input quantities. They have also tested how the choice of the parameter D in eq 10 affects the shape of the adiabatic connection curve. They found that the original metaGGA choice used in ref 4 does not yield accurate results, whereas the parameter D used here was found to yield rather accurate results up to 10 bohr.

In Figure 7, we report the dissociation curves of the H_2 and N_2 molecules in a spin-restricted formalism for different methods. Our ISI results are not very accurate if compared to the reference CCSD(T) results but qualitatively better than MP2 and B2PLYP which diverge for large distance. The inaccuracy of our ISI results originates form the approximated LHF (or HF) densities, orbitals, and orbital energies; in fact, the spin-restricted ISI turns out to be very sensitive to the input

DOI: 10.1021/acs.jctc.6b00713
J. Chem. Theory Comput. 2016, 12, 4885−4896

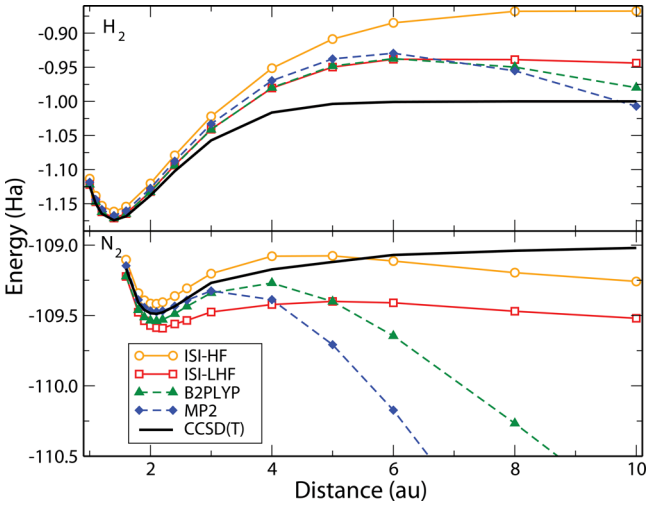

Figure 7. Dissociation energy curves for the H_2 and N_2 molecules in a spin-restricted formalism. In this case, second-order perturbation theory diverges as the molecule is stretched, and the ISI functional tends to eq 12. Note also that ISI-LHF and ISI-HF will coincide at infinite distance.

ingredients. The ISI results in ref 28 are much more accurate due to the fact that FCI input density, orbitals, and orbital energies have been used. Moreover, for H_2, we recall that the ISI results will be exact at infinite distance only if the parameter D is self-interaction free for the H atom density.[6]

5. DISCUSSION

The results reported in Section 4 show that the performance of ISI-HF is quite good when compared with HF+GGA methods (e.g., HF+PBEloc) since the former describes dynamical and static correlation without any error cancellation while the latter do not. On the other hand ISI-HF is much less appealing, if compared to MP2 which yields in many cases better results at similar computational cost. One important exception are dispersion interactions, for which ISI-HF outperforms MP2. Instead, when ISI is applied to DFT orbitals (i.e., LHF), the results are rather bad. In the following sections we try to analyze and rationalize this performance in order to provide useful information which can be used to improve functionals based on interpolations between the weak and the strong interacting limits.

5.1. Influence of the Size-Consistency Problem. Being a nonlinear function of exact exchange and GL2 total energies, the ISI xc energy functional is formally not size consistent. This means that computing the (spin-unrestricted or spin-restricted) ISI xc energy of two systems separated by a distance large enough (eventually infinite) to make the interaction between them negligible yields a result which is different form the sum of the ISI xc energies of the two isolated systems.

One exception is the case of a set of identical systems, e.g., a homonuclear dimer $A - A$, where A is closed-shell or the spin-unrestricted formalism is used. Under these conditions E_x, E_{GL2}, W_∞, and W'_∞ are all size-consistent, thus $X[A - A] = 2X[A]$, while $Y[A - A] = Y[A]$ and $Z[A - A] = Z[A]$. Since the ISI xc energy (eq 5) is linear in X and W_∞ is a size-consistent quantity, the whole result is size consistent.

The issue of size inconsistency may, of course, affect the results when atomization or interaction energies are calculated. To investigate the relevance of this problem, we perform a numerical study on the magnitude of this effect. Consider a system M (e.g., a molecule) composed of different fragments A_i (e.g., atoms) with $i = 1,..., N$. The total xc interaction energy in this system is

$$E_{xc}^{int}(M) = E_{xc}(M) - \sum_{i=1}^{N} E_{xc}(A_i) \tag{16}$$

Here, $E_{xc}(M)$ denotes the xc energy of M and $E_{xc}(A_i)$ the xc energy of the *isolated* fragment A_i. Consequently, if we denote with M^* the system obtained by bringing all fragments A_i at large distance from each other (such that their mutual interaction is negligible), this interaction energy can also be written as

$$E_{xc}^{int}(M) = E_{xc}(M) - E_{xc}(M^*) \tag{17}$$

For any size-consistent method, eqs 16 and 17 give the same result. However, for a nonsize-consistent method such as ISI, their difference

$$\Delta_{xc}(M) = E_{xc}(M^*) - \sum_{i=1}^{N} E_{xc}(A_i) \tag{18}$$

can provide a measure for the size-consistency problem (clearly, $\Delta_{xc} = 0$ for any size-consistent method).

In the specific case of ISI, we have

$$E_{xc}^{ISI}(M^*) = f^{ISI}(E_x(M^*), E_{GL2}(M^*), W_\infty(M^*), W'_\infty(M^*)) \tag{19}$$

where $f^{ISI}(w_1, w_2, w_3, w_4)$ is the nonlinear function of four variables defined in eqs 5 and 6. Assuming that all four ingredients are size consistent, we can further write

$$E_{xc}^{ISI}(M^*) = f^{ISI}\left(\sum_{i=1}^{N} E_x(A_i), \sum_{i=1}^{N} E_{GL2}(A_i), \sum_{i=1}^{N} W_\infty(A_i), \sum_{i=1}^{N} W'_\infty(A_i)\right) \tag{20}$$

Even then, we typically have $\Delta_{xc}^{ISI}(M) \neq 0$ since f^{ISI} is not linear, i.e.

$$E_{xc}^{ISI}(M^*) \neq \sum_{i=1}^{N} E_{xc}^{ISI}(A_i) \tag{21}$$

As previously mentioned, an exception arises in cases with identical fragments, $A_i = A$ (all i), since the function f^{ISI} has the property

$$f^{ISI}(Nw_1, Nw_2, Nw_3, Nw_4) = Nf^{ISI}(w_1, w_2, w_3, w_4)$$

Using eq 19 and the corresponding expression for $E_{xc}^{ISI}(A_i)$, it is possible to evaluate the effect of the size-consistency violation of ISI for different systems. The results of these calculations are reported, for a selected test set of molecules, in Table 5. In these calculations, we have considered a spin-unrestricted formalism for HF and GL2 calculations on open-shell atoms, assuming that the corresponding results are properly size consistent (whether this is formally correct is still under debate in the literature;[20] however, numerical results suggest that our approximation is quite accurate in the considered cases). Inspection of the table shows that for molecules composed of first row elements (plus hydrogen) the values of Δ_{xc} are negligible. Thus, the ISI functional behaves, in practice, as a

DOI: 10.1021/acs.jctc.6b00713
J. Chem. Theory Comput. 2016, 12, 4885−4896

Table 5. Values of Δ_{xc} per Bond (in mHa), Calculated Using Eqs 18, 19, and 20, for a Selection of Molecular Systems[a]

molecule	Δ_{xc}	molecule	Δ_{xc}
CH_4	0.03	H_2CO	0.01
NH_3	0.03	HOOH	0.02
H_2O	0.04	SiH_2	0.00
FH	0.04	PH_3	0.00
HCN	0.01	SO_2	−2.44
CO	−0.02	HCl	0.00
C_2H_4	0.02	PN	−1.39
SiC	−1.70	SiO	−3.43
PO	−3.25	NCl_3	−1.33

[a]Note that since E_x is a size-consistent quantity, $\Delta_{xc} = \Delta_c$.

size-consistent method. On the other hand, for molecules including both first and second row elements, larger values are found. We remark that these values are, anyway, often smaller than few mHa per bond, so that the size-inconsistency problem is not too large also in these cases.

The difference between the two kinds of behaviors observed in Table 5 traces back to the fact that when only first row elements are present all atoms display quite similar values of exchange and GL2 correlation; thus, the ISI behavior is rather similar to the ideal case of identical systems and the size-consistency violation is small. On the contrary, when both first and second row atoms are present, the atomic properties are significantly different and the nonlinear nature of the ISI formula leads to a non-negligible size inconsistency. Further evidence of this fact is given in Figure 8, where we report the

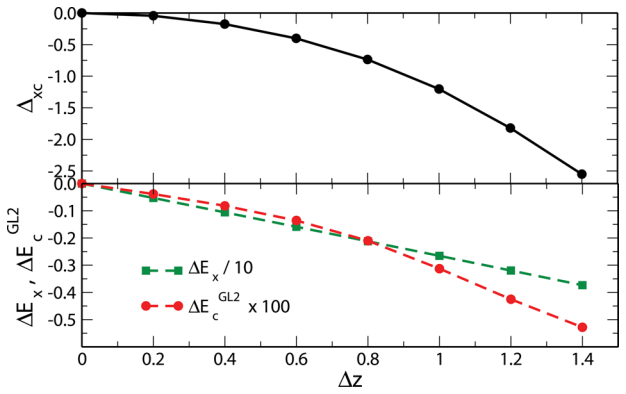

Figure 8. Upper panel: Values of Δ_{xc} as functions of ΔZ for the dissociation of N_2 into two atomic fragments having seven electrons and nuclear charges $Z_1 = 7 + \Delta Z$ and $Z_2 = 7 - \Delta Z$. Lower panel: Values of $\Delta E_x = E_x[fragment1] - E_x[fragment2]$ and $\Delta E_c^{GL2} = E_c^{GL2}[fragment1] - E_c^{GL2}[fragment2]$ as functions of ΔZ. The values of ΔE_x and ΔE_c^{GL2} have been scaled only for graphical reasons.

values of Δ_{xc} for the atomization of a N_2 molecule into two atomic fragments having sevenelectrons each (as the N atom), but nuclear charges $Z_1 = 7 + \Delta Z$ and $Z_2 = 7 - \Delta Z$, for various values of ΔZ. Indeed, the plot clearly shows that the size-consistency problem grows with the difference between the two atomic fragments.

5.2. Role of the Energy Gap. The fact that similar trends are observed in Tables 1 and 2 for ISI and GL2 correlation energies for different reference orbitals and different systems suggests that the energy gap between occupied and unoccupied molecular orbitals may play a major role in determining the accuracy of the ISI correlation energy. This difference is in fact smaller for semilocal DFT (PBE) and larger for HF, having intermediate values for hybrid and the LHF methods. Similarly, the energy gap is larger for closed shell atoms and smaller for open-shell atoms and molecules. These observations fit well with the behavior reported in Table 1 and Figure 4.

To investigate this feature, we have considered for all the systems in Table 1 the application to the LHF ground-state orbitals of a *scissor operator* to rigidly move all the unoccupied orbitals up in energy by

$$\Delta E = \alpha(E_g[\mathrm{HF}] - E_g[\mathrm{LHF}]) \tag{22}$$

where $E_g[HF]$ and $E_g[LHF]$ are the HOMO−LUMO gaps for HF and LHF, respectively, while α is a parameter used to tune the effect. Thus, for $\alpha = 0$, no shift is applied, whereas for $\alpha = 1$ the applied shift is such that the LHF HOMO−LUMO gap is lifted up to the HF value.

In the bottom panel of Figure 9, we report the deviations from reference values of the ISI correlation energies of the N_2

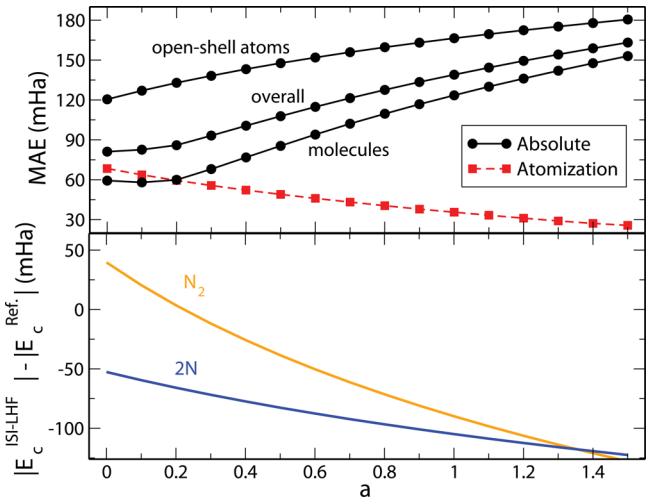

Figure 9. Top panel: Mean absolute errors (MAEs) for the ISI correlation and atomization correlation energies of the systems of Table 1 as functions of the α parameter of eq 22. Bottom panel: Deviations from reference values of the ISI correlation energies of the N_2 molecule and two N atoms as functions of the α parameter of eq 22. All results were computed using a cc-pV5Z basis set.

molecule and twice the N atom, as functions of the α parameter of eq 22. The atomization correlation energy error is thus the difference between these two curves. For simplicity, we considered here results with the 5Z basis set and not the extrapolated CBS ones. Hence, even at $\alpha = 0$, the results for N_2 are slightly different from the ones reported in Tables 1 and 2. At $\alpha = 0$, we have an atomization correlation energy error of about 100 mHa. When α is increased, the absolute correlation energies decrease due to an increased energy in the denominator. However, the slopes of the lines are different. At $\alpha \approx 1$ (i.e at the HF gap), the two lines almost cross, meaning that the ISI-HF method yields the correct atomization correlation energy.

The MAEs computed for different values of the parameter α for the ISI correlation energies of open-shell atoms, molecules, and both, as well as the MAE of the correlation atomization energies, are reported in the upper panel of Figure 9. The plot shows that the application of a shift for the unoccupied orbitals generally leads to a worsening of the ISI correlation energies.

DOI: 10.1021/acs.jctc.6b00713
J. Chem. Theory Comput. 2016, 12, 4885−4896

This is particularly true for atoms, which already suffer for an underestimation (in absolute value) of the correlation energy, thus increasing the energy difference between occupied and virtual orbitals adds a further underestimation. For molecules instead at low values of α, a moderate improvement of the correlation energy is observed since in most molecules LHF-ISI overestimates (in absolute value) correlation energies that are thus improved by the application of a shift. Nevertheless, for larger values of α in all molecules an underestimation of the correlation is found, so the results rapidly worsen with increasing shift. We note that the rate of worsening for molecular correlation energies is quite faster that that observed for atoms.

5.3. Dispersion Interactions. The good performance of the ISI-HF for dispersion interactions is surprising and deserves further thoughts. First of all, we notice that the functional $E_{xc}^{ISI}[\rho]$ defined by eqs 5−10 inherits (at least for the case of equal fragments) the long-range $\sim R^{-6}$ dispersion interaction energy dependence from its E_{GL2} component (MP2 in the case of HF reference orbitals considered here). Yet, it systematically outperforms MP2, suggesting that it adds a sensible correction to it. The analysis of Strømsheim et al.[94] shows that the adiabatic connection curve for the interaction energy of dispersion complexes deviates significantly from the linear behavior, requiring a considerable amount of "nondynamical" correlation, which seems to be well accounted for by the ISI functional (although the picture may be different with HF orbitals).

A possible explanation may be derived by looking at the functional $W'_\infty[\rho]$, which describes the physics of coupled oscillations of localized electrons. Its PC semilocal approximation of eq 10 is a quantitatively good approximation of this energy.[8] The physics of dispersion interactions is actually very similar, describing oscillations of coupled charge fluctuations on the two fragments. We suspect that when looking at the interaction energy, the physics introduced by $W'_\infty[\rho]$ (when subtracting the internal part of each fragment) is actually correct. However, a more detailed study of this aspect is required, and it will be the object of our future work.

6. CONCLUSIONS AND PERSPECTIVES

We have reported the first detailed study of the performances of a functional that includes (in an approximate way) the strong-coupling limit, analyzing its dependence on basis set, reference orbitals, and other aspects such as the size consistency error. Overall, the ISI functional has serious limitations, which could have been expected from some of its formal deficiencies. We have rationalized our findings, providing useful information for functionals that can retain the information from the strong-coupling limit while remedying to these deficiencies.[22] In future work, we plan to extend our analysis to functionals based on local interpolations along the adiabatic connection,[15,22−26] implementing the needed input quantities.

An unexpected finding that emerged from our study is a very good performance of the ISI functional (when used as a correction to Hartree−Fock) for dispersion interactions, yielding a mean absolute error of only 0.4 kcal/mol on the S22 set, and consistently improving over MP2 in a significative way for dispersion complexes (Figures 5 and 6). We suspect that the functional $W'_\infty[\rho]$, which describes coupled oscillations of localized electrons, is able to capture the physics of interaction energy in dispersion complexes. This is an interesting perspective for the ISI functional, which we will investigate in detail in a future work.

AUTHOR INFORMATION

Corresponding Author

*E-mail: eduardo.fabiano@nano.cnr.it.

Notes

The authors declare no competing financial interest.

ACKNOWLEDGMENTS

We thank Evert Jan Baerends, Oleg Gritsenko, and Stefan Vuckovic for insightful discussions and TURBOMOLE GmbH for providing the TURBOMOLE program. P.G.-G. and M.S. acknowledge the European Research Council under H2020/ERC Consolidator Grant corr-DFT [Grant 648932] for financial support.

REFERENCES

(1) Wigner, E. P. *Phys. Rev.* **1934**, *46*, 1002.
(2) Wigner, E. P. *Trans. Faraday Soc.* **1938**, *34*, 678.
(3) Seidl, M.; Perdew, J. P.; Levy, M. *Phys. Rev. A: At., Mol., Opt. Phys.* **1999**, *59*, 51.
(4) Seidl, M.; Perdew, J. P.; Kurth, S. *Phys. Rev. Lett.* **2000**, *84*, 5070.
(5) Seidl, M. *Phys. Rev. A: At., Mol., Opt. Phys.* **1999**, *60*, 4387.
(6) Seidl, M.; Perdew, J. P.; Kurth, S. *Phys. Rev. A: At., Mol., Opt. Phys.* **2000**, *62*, 012502.
(7) Seidl, M.; Gori-Giorgi, P.; Savin, A. *Phys. Rev. A: At., Mol., Opt. Phys.* **2007**, *75*, 042511.
(8) Gori-Giorgi, P.; Vignale, G.; Seidl, M. *J. Chem. Theory Comput.* **2009**, *5*, 743.
(9) Buttazzo, G.; De Pascale, L.; Gori-Giorgi, P. *Phys. Rev. A: At., Mol., Opt. Phys.* **2012**, *85*, 062502.
(10) Cotar, C.; Friesecke, G.; Klüppelberg, C. *Comm. Pure Appl. Math.* **2013**, *66*, 548.
(11) Malet, F.; Gori-Giorgi, P. *Phys. Rev. Lett.* **2012**, *109*, 246402.
(12) Mirtschink, A.; Seidl, M.; Gori-Giorgi, P. *Phys. Rev. Lett.* **2013**, *111*, 126402.
(13) Mendl, C. B.; Malet, F.; Gori-Giorgi, P. *Phys. Rev. B: Condens. Matter Mater. Phys.* **2014**, *89*, 125106.
(14) Wagner, L. O.; Gori-Giorgi, P. *Phys. Rev. A: At., Mol., Opt. Phys.* **2014**, *90*, 052512.
(15) Zhou, Y.; Bahmann, H.; Ernzerhof, M. *J. Chem. Phys.* **2015**, *143*, 124103.
(16) Odashima, M. M.; Capelle, K. *Phys. Rev. A: At., Mol., Opt. Phys.* **2009**, *79*, 062515.
(17) Karolewski, A.; Kronik, L.; Kümmel, S. *J. Chem. Phys.* **2013**, *138*, 204115.
(18) Mori-Sanchez, P.; Cohen, A. J.; Yang, W. T. *J. Chem. Phys.* **2006**, *124*, 091102.
(19) Gori-Giorgi, P.; Savin, A. *J. Phys.: Conf. Ser.* **2008**, *117*, 012017.
(20) Savin, A. *Chem. Phys.* **2009**, *356*, 91.
(21) Mirtschink, A.; Seidl, M.; Gori-Giorgi, P. *J. Chem. Theory Comput.* **2012**, *8*, 3097.
(22) Vuckovic, S.; Irons, T. J. P.; Savin, A.; Teale, A. M.; Gori-Giorgi, P. *J. Chem. Theory Comput.* **2016**, *12*, 2598−2610.
(23) Kong, J.; Proynov, E. *J. Chem. Theory Comput.* **2016**, *12*, 133−143.
(24) Becke, A. D. *J. Chem. Phys.* **2013**, *138*, 074109.
(25) Becke, A. D. *J. Chem. Phys.* **2013**, *138*, 161101.
(26) Becke, A. D. *J. Chem. Phys.* **2013**, *139*, 021104.
(27) Malet, F.; Mirtschink, A.; Cremon, J. C.; Reimann, S. M.; Gori-Giorgi, P. *Phys. Rev. B: Condens. Matter Mater. Phys.* **2013**, *87*, 115146.
(28) Teale, A. M.; Coriani, S.; Helgaker, T. *J. Chem. Phys.* **2010**, *132*, 164115.
(29) Malet, F.; Mirtschink, A.; Giesbertz, K.; Wagner, L.; Gori-Giorgi, P. *Phys. Chem. Chem. Phys.* **2014**, *16*, 14551−14558.

DOI: 10.1021/acs.jctc.6b00713
J. Chem. Theory Comput. 2016, 12, 4885−4896

(30) Mirtschink, A.; Umrigar, C. J.; Morgan, J. D.; Gori-Giorgi, P. *J. Chem. Phys.* **2014**, *140*, 18A532.
(31) Vuckovic, S.; Wagner, L. O.; Mirtschink, A.; Gori-Giorgi, P. *J. Chem. Theory Comput.* **2015**, *11*, 3153−3162.
(32) Langreth, D. C.; Perdew, J. P. *Solid State Commun.* **1975**, *17*, 1425.
(33) Görling, A.; Levy, M. *Phys. Rev. A: At., Mol., Opt. Phys.* **1994**, *50*, 196.
(34) Mendl, C. B.; Lin, L. *Phys. Rev. B: Condens. Matter Mater. Phys.* **2013**, *87*, 125106.
(35) Chen, H.; Friesecke, G.; Mendl, C. B. *J. Chem. Theory Comput.* **2014**, *10*, 4360−4368.
(36) Liu, Z. F.; Burke, K. *J. Chem. Phys.* **2009**, *131*, 124124.
(37) Cohen, A. J.; Mori-Sanchez, P.; Yang, W. *Science* **2008**, *321*, 792.
(38) Yang, W.; Mori-Sanchez, P.; Cohen, A. J. *J. Chem. Phys.* **2013**, *139*, 104114.
(39) Garza, A. J.; Scuseria, G. E.; Ruzsinszky, A.; Sun, J.; Perdew, J. P. *Mol. Phys.* **2016**, *114*, 928.
(40) Perdew, J. P.; Burke, K.; Ernzerhof, M. *Phys. Rev. Lett.* **1996**, *77*, 3865.
(41) Adamo, C.; Barone, V. *J. Chem. Phys.* **1999**, *110*, 6158−6170.
(42) Perdew, J. P.; Ernzerhof, M.; Burke, K. *J. Chem. Phys.* **1996**, *105*, 9982−9985.
(43) Becke, A. D. *J. Chem. Phys.* **1993**, *98*, 1372.
(44) Becke, A. D. *Phys. Rev. A: At., Mol., Opt. Phys.* **1988**, *38*, 3098.
(45) Lee, C.; Yang, W.; Parr, R. G. *Phys. Rev. B: Condens. Matter Mater. Phys.* **1988**, *37*, 785.
(46) Della Sala, F.; Görling, A. *J. Chem. Phys.* **2001**, *115*, 5718−5732.
(47) Gritsenko, O. V.; Schipper, R. R. T.; Baerends, E. J. *J. Chem. Phys.* **1997**, *107*, 5007.
(48) Dunning, T. H. *J. Chem. Phys.* **1989**, *90*, 1007.
(49) Kendall, R. A.; Dunning, T. H.; Harrison, R. J. *J. Chem. Phys.* **1992**, *96*, 6796−6806.
(50) Woon, D. E.; Dunning, T. H. *J. Chem. Phys.* **1993**, *98*, 1358−1371.
(51) Woon, D. E.; Dunning, T. H. *J. Chem. Phys.* **1994**, *100*, 2975.
(52) *TURBOMOLE, V6.3*; TURBOMOLE GmbH: Karlsruhe, Germany, 2011. http://www.turbomole.com (accessed November 2015)
(53) Furche, F.; Ahlrichs, R.; Hättig, C.; Klopper, W.; Sierka, M.; Weigend, F. *WIREs Comput. Mol. Sci.* **2014**, *4*, 91.
(54) Lynch, B. J.; Truhlar, D. G. *J. Phys. Chem. A* **2003**, *107*, 8996.
(55) Haunschild, R.; Klopper, W. *Theor. Chem. Acc.* **2012**, *131*, 1112.
(56) Curtiss, L. A.; Raghavachari, K.; Redfern, P. C.; Pople, J. A. *J. Chem. Phys.* **1997**, *106*, 1063−1079.
(57) Haunschild, R.; Klopper, W. *J. Chem. Phys.* **2012**, *136*, 164102.
(58) Lynch, B. J.; Zhao, Y.; Truhlar, D. G. *J. Phys. Chem. A* **2003**, *107*, 1384−1388.
(59) Goerigk, L.; Grimme, S. *J. Chem. Theory Comput.* **2010**, *6*, 107−126.
(60) Goerigk, L.; Grimme, S. *Phys. Chem. Chem. Phys.* **2011**, *13*, 6670−6688.
(61) Zhao, Y.; Lynch, B. J.; Truhlar, D. G. *J. Phys. Chem. A* **2004**, *108*, 2715−2719.
(62) Zhao, Y.; González-García, N.; Truhlar, D. G. *J. Phys. Chem. A* **2005**, *109*, 2012−2018.
(63) Lynch, B. J.; Truhlar, D. G. *J. Phys. Chem. A* **2003**, *107*, 3898.
(64) Zhao, Y.; Truhlar, D. G. *J. Chem. Theory Comput.* **2005**, *1*, 415.
(65) Fabiano, E.; Constantin, L.; Della Sala, F. *J. Chem. Theory Comput.* **2014**, *10*, 3151−3162.
(66) Jurečka, P.; Šponer, J.; Černỳ, J.; Hobza, P. *Phys. Chem. Chem. Phys.* **2006**, *8*, 1985−1993.
(67) Marshall, M. S.; Burns, L. A.; Sherrill, C. D. *J. Chem. Phys.* **2011**, *135*, 194102.
(68) Müller, T. Basis Set Accuracy and Calibration in Quantum Chemistry. In *Computational Nanoscience: Do It Yourself!*; Grotendorst, J., Blugel, S., Marx, D., Eds.; NIC Series, Volume *31*; John von Neumann Institute for Computing: Julich, 2006; pp 19−43.
(69) Truhlar, D. G. *Chem. Phys. Lett.* **1998**, *294*, 45−48.
(70) Bakowies, D. *J. Chem. Phys.* **2007**, *127*, 164109.
(71) Varandas, A. J. C. *J. Chem. Phys.* **2007**, *126*, 244105.
(72) Feller, D.; Peterson, K. A.; Grant Hill, J. *J. Chem. Phys.* **2011**, *135*, 044102.
(73) Fabiano, E.; Della Sala, F. *Theor. Chem. Acc.* **2012**, *131*, 1278.
(74) Fast, P. L.; Sánchez, M. L.; Truhlar, D. G. *J. Chem. Phys.* **1999**, *111*, 2921−2926.
(75) Janesko, B. G.; Scuseria, G. E. *J. Chem. Phys.* **2008**, *128*, 084111.
(76) Kim, M.-C.; Park, H.; Son, S.; Sim, E.; Burke, K. *J. Phys. Chem. Lett.* **2015**, *6*, 3802−3807.
(77) Grimme, S. *J. Chem. Phys.* **2006**, *124*, 034108.
(78) Jankowski, K.; Grabowski, I.; Nowakowski, K.; Wasilewski, J. *Collect. Czech. Chem. Commun.* **2005**, *70*, 1157.
(79) Fabiano, E.; Della Sala, F. *J. Chem. Phys.* **2007**, *126*, 214102.
(80) Grabowski, I.; Teale, A. M.; Śmiga, S.; Bartlett, R. J. *J. Chem. Phys.* **2011**, *135*, 114111.
(81) Grabowski, I.; Teale, A. M.; Fabiano, E.; Śmiga, S.; Buksztel, A.; Della Sala, F. *Mol. Phys.* **2014**, *112*, 700−710.
(82) Rohr, D.; Gritsenko, O.; Baerends, E. J. *Chem. Phys. Lett.* **2006**, *432*, 336.
(83) Constantin, L. A.; Fabiano, E.; Della Sala, F. *Phys. Rev. B: Condens. Matter Mater. Phys.* **2012**, *86*, 035130.
(84) Gritsenko, O. V.; Schipper, P. R. T.; Baerends, E. J. *J. Chem. Phys.* **1997**, *107*, 5007−5015.
(85) Handy, N. C.; Cohen, A. J. *Mol. Phys.* **2001**, *99*, 403−412.
(86) O'Neill, D. P.; Gill, P. M. W. *Mol. Phys.* **2005**, *103*, 763−766.
(87) Becke, A. D. *J. Chem. Phys.* **2005**, *122*, 064101.
(88) Fabiano, E.; Trevisanutto, P. E.; Terentjevs, A.; Constantin, L. A. *J. Chem. Theory Comput.* **2014**, *10*, 2016−2026.
(89) Rezác, J.; Riley, K. E.; Hobza, P. *J. Chem. Theory Comput.* **2011**, *7*, 2427−2438.
(90) Rezác, J.; Riley, K. E.; Hobza, P. *J. Chem. Theory Comput.* **2012**, *8*, 4285−4292.
(91) Grabowski, I.; Fabiano, E.; Della Sala, F. *Phys. Chem. Chem. Phys.* **2013**, *15*, 15485−15493.
(92) Fabiano, E.; Della Sala, F.; Grabowski, I. *Chem. Phys. Lett.* **2015**, *635*, 262−267.
(93) Gráfová, L.; Pitonák, M.; Rezác, J.; Hobza, P. *J. Chem. Theory Comput.* **2010**, *6*, 2365−2376.
(94) Strømsheim, M. D.; Kumar, N.; Coriani, S.; Sagvolden, E.; Teale, A. M.; Helgaker, T. *J. Chem. Phys.* **2011**, *135*, 194109.

DOI: 10.1021/acs.jctc.6b00713
J. Chem. Theory Comput. 2016, 12, 4885−4896